Orthodontics & Craniofacial Research

ORIGINAL ARTICLE

G. R. S. Naveh
S. Weiner

Initial orthodontic tooth movement of a multirooted tooth: a 3D study of a rat molar

Authors' affiliation:
G. R. S. Naveh, S. Weiner, Department of Structural Biology, Weizmann Institute of Science, Rehovot, Israel

Correspondence to:
G. R. S Naveh
Department of Structural Biology
Weizmann Institute of Science
76100 Rehovot, Israel
E-mail: dr.naveh@gmail.com

Naveh G. R. S., Weiner S. Initial orthodontic tooth movement of a multirooted tooth: a 3D study of a rat molar
Orthod Craniofac Res 2015; **18**: 134–142. © 2015 John Wiley & Sons A/S. Published by John Wiley & Sons Ltd

Structured Abstract

Objective – To elucidate the 3D interactions in the tooth–PDL–bone complex immediately after application of orthodontic forces and their implications on tooth movement and function.

Methods – A special visualization method using microCT allows us to directly image in 3D the movements of a multirooted molar tooth inside the alveolar bone as well as the collagenous network of the PDL. Using fresh, unstained rat mandibular 1st molar under mesial loads of 0.5–1 N, we address basic concepts in orthodontics during the initial stages of orthodontic movement.

Results – We show that immediately after the application of orthodontic load, direct distinct contacts between the tooth and the bone form in the furcation area. These contacts limit tooth movement and interfere with whole body translation. Only localized sites of highly compressed PDL between the root surfaces and the bone were observed. In general, the collagenous network of the PDL appeared loose and not densely packed in the compressed side. On the tension side, the fibers maintained their overall orientation without any significant extension of the fibers.

Conclusions – Localized direct contact areas between the tooth roots and the bone at the furcation already form within a few minutes of orthodontic tooth movement. This direct and localized bone involvement guides the movement trajectory and provides a mechanism for the miscorrelation found between force levels and tooth movement during the initial stages of an orthodontic tooth movement.

Key words: initial orthodontic movement; microCT; molar; multirooted tooth movement; PDL

Date:
Accepted 6 December 2014

DOI: 10.1111/ocr.12066

Introduction

Tooth movement is an important strategy for tooth survival in response to loads (1, 2). Orthodontic tooth movement on the

other hand intervenes with natural tooth function. Ideally, the orthodontically moving tooth should maintain its basic functionality. However, the instantaneous change in the tooth location at the first moment of force application in the orthodontic treatment already affects tooth function. This study aims at elucidating the mechanism of tooth movement by tracking the structural changes in the tooth–PDL–bone complex during the initial stages of orthodontic load application in a multirooted tooth model. This sheds light on how orthodontic treatment may affect tooth function. We use a unique 3D visualization technique inside a microCT to visualize in 3D the *in situ* fresh tooth–PDL–bone complex in its native state without fixation, slicing, or staining with contrast enhancement agents (3, 4).

There is consensus that orthodontic tooth movement is directly associated with bone remodeling, as first suggested by Sandstedt and Oppenheim (5–7). However, the trigger for such remodeling is still debated (6). One hypothesis is the creation of tension and compression forces inside the PDL and is based on the assumption that no direct contacts are formed between the tooth root and the alveolar bone (5, 7).

Baumrind suggested another mechanism triggering bone remodeling: the bone-bending hypothesis (8). Mühlemann was probably the first to prove that direct involvement of bone deformation during tooth physiological function exists (9). In an *in vivo* experiment, he produced force-displacement curves for a reimplanted incisor that lacked the PDL tissue, as well as for the adjacent intact incisor of a young human male. The difference between the curves was only at the initial stage due to the absence of the PDL. Direct contact between the tooth root and alveolar bone during orthodontic tooth movement was also shown by Gottlieb (10). Gottlieb stated that the contact with the bone, during the initial stages of tooth movement, is the limiting factor for any further tooth movement. Baumrind subsequently proposed that the bone does not fully stop the movement, but undergoes deflection during orthodontic tooth movement (8). Direct evidence for the formation of specific contact areas between the root surface and the alveolar bone under physiological functional loads was obtained in a 3D study using a rat 1st mandibular molar (M1) (11).

Determination of the optimal force for the most efficient orthodontic movement has been the aim of many studies. To date, no such value is known. Reasons for this are our lack of understanding of the mechanism that guides the movement and the 3D changes that occur to the tooth–PDL–bone complex due to the orthodontic force. Moreover, the 3D structures of a single-rooted tooth and a multirooted tooth are very different; an issue barely addressed in the literature. Clinically, bone resorption in the furcation area of multirooted teeth is known to be an indicator for early stages of periodontal disease as well as for overload on teeth and parafunction. The involvement of the furcation in orthodontic movement, however, has not been addressed. It was shown (11) that under vertical functional loads, localized contact areas between the tooth and the bone are formed at the furcation. The furcation therefore serves as a fulcrum on which the tooth rotates. We hypothesize that the furcation has a central role in orthodontic tooth movement as well.

Here we address three questions relating to initial orthodontic movement of a multirooted tooth: 1) Does direct tooth–bone contact form under orthodontic loads? 2) What is the 3D movement of a multirooted tooth under initial orthodontic force? 3) What happens to the collagenous network arrangement under orthodontic loads?

Materials and methods

Animals

The study was approved by the IACUC at the Weizmann Institute of Science. Twelve 15-week-old Wistar rats (Harlan Laboratories, Israel) were fed a diet of hard pellets with water *ad libitum*. They were sacrificed by decapitation to ensure minimal changes to the PDL tissue. The mandible was immediately

excised and cut at the fibrous mandibular symphysis into two hemi-mandibles. Each hemi-mandible, containing three intact molars and one incisor, was kept in a sealed humidified tube. Within 30 min after the sacrifice, the hemi-mandible was mounted inside the microCT.

Loading procedure and micro-computed tomography (microCT)

A custom-made computer-controlled loading device was used. For details, see Naveh et al. (11) (Fig. 1A). Briefly, the device is composed of a fixed stage and a vertically moving anvil inside a cylindrical humidity chamber that is inserted into a microCT. The freshly dissected hemi-mandible was bonded to the fixed stage inside the humidity chamber using a dental restorative composite material, Z100™ (3M ESPE, compressive yield strength 470 N/mm^2). Then a short tomographic scan was made prior to the orthodontic loading in order to obtain 3D structural information regarding the tooth–PDL–bone complex prior to applying the orthodontic load. The scan time was reduced to 66 min to minimize tissue deterioration changes. To produce a mesial movement, a copper round wire with a diameter of 0.25 mm was slotted between the mandibular M1 and M2 and wrapped around the M1. The wire was connected to either an orthodontic NiTi spring (Forestadent, Germany) (Fig. 1B,C) or to an elastic power chain (American Orthodontics, Wisconsin, USA) (Fig. 1D). The orthodontic spring or elastic power chain was then stretched and anchored to the mandibular incisor (Fig. 1B–D) producing a mesial load of 0.5 N (power chain) or 1 N (NiTi coil). Then, the crown of the M1 tooth was bonded to the upper anvil resulting in mechanical stabilization of the tooth and the PDL network, preventing any further movement or changes in the tooth-PDL-bone complex. A high-resolution long scan was then carried out. In order to verify that no drastic changes occurred to the tissues during the short scan, four long scans were conducted without the preliminary short scans. Note too that any movement or structural deformation during the scan, within the scan's spatial resolution, will result in a blurred image which cannot be reconstructed or analyzed. The presented results had no distortions during the scans and therefore represent the changes in the tooth–PDL–bone complex that occurred from the time of the mesial load exertion until the hemi-mandible was mounted to the chamber (approximately 5 min).

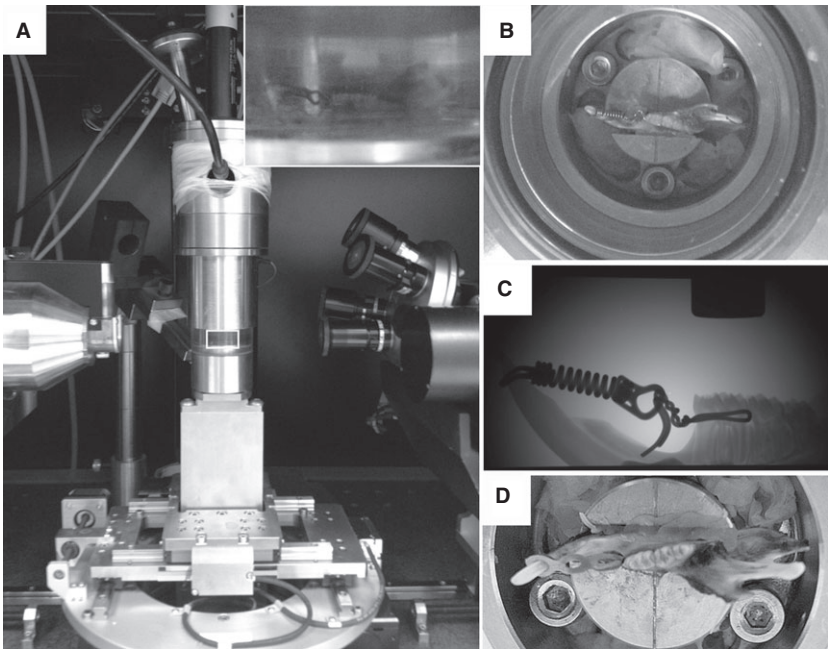

Fig 1. (A) The loading apparatus inside the microCT. Inset: (A) view through the clear window of the chamber. (B) Top view of the hemi-mandible bonded to the stage after activation of the orthodontic NiTi spring. (C) A side projection at 0.5× magnification of the hemi-mandible with the NiTi spring. (D) Specimen with an orthodontic elastic chain.

Data collection and analysis

An XRadia MICRO XCT-400 (Zeiss, California, USA) was used. A short low-resolution scan was carried out for orientation of the unloaded tooth. This was followed by a long high-resolution scan. No X-ray source filter was used.

Short scan: The microCT source was set to 40 kV and 200 μA, and 400 projection images were recorded with an exposure time of 10 s for each image. Long scan: The microCT source was set to 40 kV and 200 μA. 2500 projection images were recorded with an exposure time of 20 s for the 4× magnification lens. 25 s for the 10× magnification and for the 20× magnification 38 s.

The 3D volume was reconstructed using a back projection filtered algorithm (XRadia). Once the reconstruction of the volume was completed, 3D image processing and analysis were carried out using Avizo® software (FEI, Oregon, USA). Manual segmentation was carried out for the tooth and bone creating 3D objects. The PDL fibers were not individually segmented but were visualized using the voltex and slice tools. Registration of the scans before and after loading was made manually by overlapping the 3D segmented objects of the alveolar bone, which showed no difference when loaded in respect to the unloaded state.

Results

The orthodontic load was applied to the M1 by wrapping a copper wire around the molar just above the furcation level and pulling the tooth

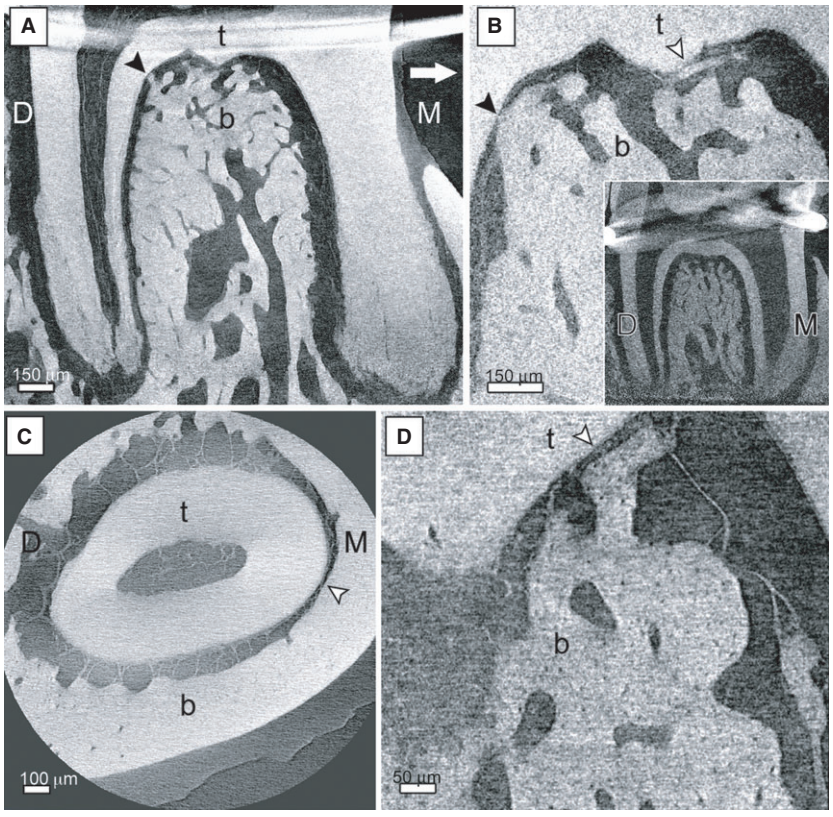

Fig. 2. M–mesial, D–distal all subfigures are oriented in the same directions. (A) 2D sagittal view from a tomographic scan (4× magnification, 3.8 μm voxel size) of the rat M1 tooth (t) inside the alveolar bone (b) under a mesial orthodontic force showing the mesial and distal roots (white arrow shows the direction of the force). Note the difference in the PDL width on the mesial sides of the roots (compression side) in relation to the distal sides of the roots (tension side). Black arrowhead – a direct contact area between the tooth and the bone. (B) sagittal plane at 10× (1.53 μm voxel size) focusing on the furcation of the M1 showing a direct contact area between the tooth and bone (black arrowhead), as well as areas of close proximity, where dense non-fibrillar soft tissue separates the tooth and the bone (white arrowhead). Inset: 2D sagittal slice of a 4× scan of a M1 before loading. (C) 2D transverse view of the mesial root (10× magnification, 1.53 μm voxel size) showing close proximity without contact between the tooth and the bone at the mesial aspect of the root (white arrowhead). (D) 2D sagittal view of the close proximity area at the furcation (20× magnification, 0.77 μm voxel size). This image clearly shows the dense soft tissue separating the tooth (t) and the bone (t) (white arrowhead).

mesially with a force of 0.5 N or 1 N. The results presented were consistent for both force levels and for all the experimental specimens. In general, the M1 crown moved in the mesial and lingual directions. The PDL thickness changed, as expected, along the entire length of the roots (Fig. 2A – loaded and 2B inset – before loading). Direct contacts between the tooth and the alveolar bone were observed at specific areas on the furcation surface without any PDL tissue in between (Fig. 2A,B black arrowhead). Without external loads, such direct contacts do not exist (Fig. 2B inset). These contacts clearly restrict the movement of the tooth. Other larger areas, but still distinct, were also observed where the tooth roots and alveolar bone were in close proximity, but not in direct contact. Interestingly in these areas of close proximity, a particularly dense soft tissue separates the tooth and the bone (Fig. 2B–D white arrowhead).

Three dimensional analysis of the 3D tooth movement was carried out by segmenting the tooth and bone before and after loading and then manually overlapping the 3D images. The bone serves as the registration reference. This method shows the relative tooth movement caused by the orthodontic load. The 3D rendered models (Fig. 3) show a rotation movement toward the mesial and lingual directions (Fig. 3A,B). By comparing the correlated 2D slices of the tooth before and after loading, we noted that although the entire tooth moves in the mesial direction, the extent of the movement is larger on the coronal side than the apical side (a controlled tipping movement). Figure 3C,D shows that the apex of the distal root hardly moved, whereas the furcation area moved about 50 microns toward the mesial direction until a contact between the tooth and the bone formed (Fig. 3C,D red arrows). This movement indicates that a controlled tipping movement of the tooth occurred with a center of rotation around the apical region of the distal root.

Using our custom-made visualization setup (4), we were also able to track the PDL collagenous network deformation that occurred immediately after mesial movement of the M1 *in situ*,

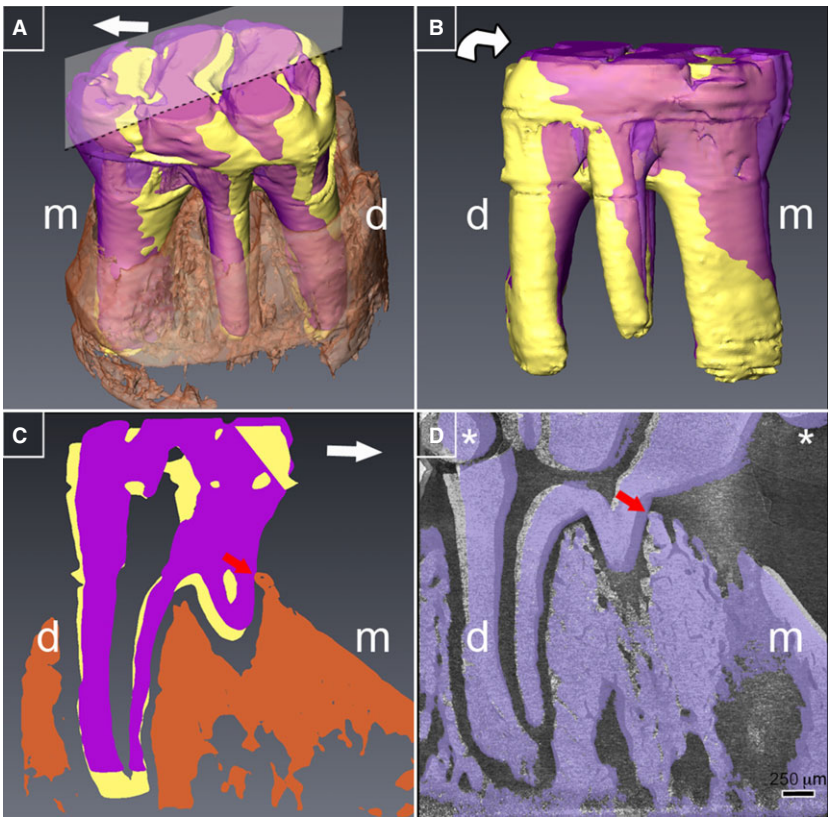

Fig. 3. 3D volume rendering of the tooth before movement (yellow) and after movement (purple). (A) Top lingual view showing that the crown moves much more in the mesial direction than the root apices. (B) Buccal view demonstrating the differential lingual and mesial movements of the tooth. The curved arrow shows the overall direction of tooth movement. (C) 2D view in the sagittal plane (as drawn in A) demonstrating a contact area (red arrow) at the furcation near the lingual root. (D) 2D overlapping views before (gray levels) and after mesial (purple) loading. Here, a wire (marked with asterisks) was slotted inside a canal drilled within the tooth at the distal aspect and serves as a reference. Note the minimal movement of the distal root apical aspect and the evident movement of the crown demonstrated also by the change in the wire location. Note the contact area formed at the furcation (red arrow).

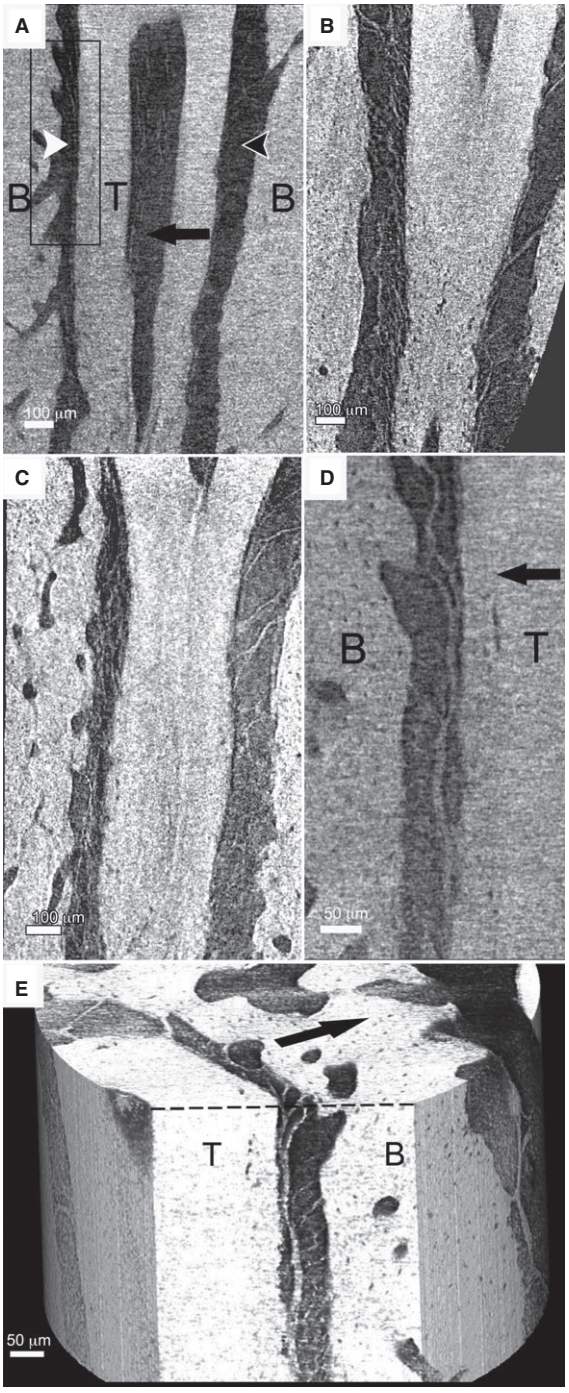

Fig. 4. (A–D): 2D sagittal views of the buccal root. (A) Black arrow shows the direction of the mesial force. Note the narrow PDL space at the mesial aspect of the root (white arrowhead) and the relatively wide uniform PDL space on the distal aspect of the root (black arrowhead). T–tooth, B–bone. (B) Unloaded tooth, showing the PDL collagenous networks: sparse network on the right and dense network on the left. (C) Loaded tooth, showing the PDL collagenous networks: dense network on the left which is also the compression side. The sparse network is located on the right. (D) Higher magnification scan (20×, 0.77 μm voxel size) of the area marked in A with a rectangle. This shows the fiber orientations in the compression side. Note the loose form of the fibers. (E) 3D volume rendering of the tooth and the bone in the compression side.

without the use of any sectioning, fixation, or staining, that is, in its native state. Figure 4A shows the buccal root of the rat M1 five minutes after application of the mesial load. Note the relatively narrow PDL space on the mesial side (compression side, white arrowhead) when compared to the distal side (tension side, black arrowhead). A comparison of the overall collagenous network orientation without loading (Fig. 4B) and after loading (Fig. 4C) shows the presence of a dense network of collagenous sheets on the compressed side. On the tension side, however, the collagenous network structure is similar to the unloaded state. A scan at higher magnification of the mesial PDL space shows that the PDL collagenous fibers in the compressed side are loose and not densely packed (Fig. 4D,E).

Discussion

We investigated the initial orthodontic tooth movement of a multirooted rat M1. We also visualized in 3D the structural changes of the tooth-PDL-bone complex immediately after orthodontic loading of 0.5 N and 1 N. Note that the rat M1 has a crown-apex length of about 3 mm and an M-D crown length of about 2.5 mm, which is about therefore can be estimated as 1/7 the size of a human M1 (12) and not 1/50 as previously claimed (13). Taking into consideration the fact that the rat M1 has 4 roots as opposing to 2 roots in a human molar and a mean PDL width of about 100 microns which is about third of that of the human PDL (14), a load of about 0.5–1 N is definitely within the orthodontic force range for this specimen (15). We show that both magnitudes of the orthodontic force result in direct contacts between the tooth and the alveolar bone similar to those that appear under higher vertical functional loads. These direct contacts prevent further gross movement of the tooth, as was previously assumed by Gotlieb (10) and Baumrind (8) and explain the fact that an increase of orthodontic forces does not result in a greater tooth movement (16, 17).

The role of the furcation

A previous study of the rat M1 (11) showed that a vertical compression load moved the tooth until it contacted the alveolar bone at the furcation. Localized specific contact areas between the roots and the bone were observed in the furcation when the force exceeded 10 N. Therefore, the furcation has an important role as it functions as a limiting factor for tooth movements under functional loads and serves as a fulcrum around which the tooth rotates. Here we show that under much lower loads of 0.5 N and 1 N but applied in a mesial direction, similar contact areas form between the tooth and the bone in the furcation. We also show that despite the mesial direction of the applied force, no direct contacts between the roots and the bone are observed along the mesial sides of the roots. Therefore, it can be said that the furcation has a unique role in guiding and limiting the tooth movement both in physiological and orthodontic loading.

In this study, we were careful to dissect the mandible in the fibrous symphysis and therefore leave the hemi-mandible structurally intact. In addition, the samples were fresh and loaded within minutes after sacrifice. The major drawback of the experimental system used is the lack of blood pressure. However, previous studies showed that the values of blood pressure in the PDL resistance are as small as 1 mmHg (1.35 g/cm^2) (18), which are negligible in relation to forces of 0.5 N or 1 N on a surface area of about 50 mm^2 (100–200 g/cm^2) used here and in orthodontics in general. We are therefore of the opinion that also *in vivo*, the orthodontic forces result in direct contact between the tooth and bone at the furcation. This overload at the furcation might lead to an inflammation similar to that encountered during traumatic occlusion. This possibility should be further investigated. In our study, contact areas along the roots were not observed. However, we did observe areas where the root and bone surfaces were in close proximity immediately after initial movement. With additional mastication loads, the areas of closest proximity may become direct contact areas. The additive influence of functional and habitual forces to the areas of contact and areas of close proximity is therefore crucial in orthodontic tooth movement and should also be further investigated. The alveolar bone at the furcation is clearly not compact, but is surprisingly porous compared to the other areas of the alveolus. It will be interesting to understand the detailed structure of this bone, as well as a possible sensing function by the cells in this area. Moreover, an important question regards the fate of the cells and the collagenous network at sites of direct contact should be addressed in future studies, as well as whether there is a correlation between the contact areas and the hyalinization phenomenon (area which lacks cells and collagen fibers).

Movement direction

Whole body movement of a tooth was defined by Reitan as a movement where the whole 'side' of the root moves (19) and therefore the force that is transferred to the bone is distributed over the entire 'side' of the root. Here our 2D observations show a uniform change in the width of the PDL, which is characteristic of whole body movement. The analysis of the 3D movements, however, reveals that the tooth is not translating and is in fact tipping toward the mesial and lingual directions. We show that in an initial orthodontic movement of a multirooted tooth, using a round wire, pure translation of the tooth does not occur and estimation of tooth movement based on 2D images is questionable. Moreover, here the distal root apex serves as a pivot around which the tooth rotates—the center of rotation. We surmise that after the contact at furcation is formed, the center of rotation is located in the furcation area. Studies investigating strains in the PDL during orthodontic tooth movement, mainly based on finite element analysis (FEA) (20, 21) showed a non-uniform stress distribution along the root. Some studies concluded that the cervical region is a high stress bearing area (22, 23). However, no study to date relates to the furcation as a load-bearing area. It would be interesting though to analyze the 3D movement of a multirooted tooth moved with a coupled force device that is

designed to generate a root torque or pure bodily movement of a tooth. We assume that even then contacts between the tooth and the bone will form in the furcation and a uniform distribution of the load never occurs. This should be also further investigated in relation to surgical methods for accelerated orthodontic tooth movement.

PDL

An examination of the PDL collagenous network on the compressed side, namely the mesial aspects of the roots, shows that the collagen fibers are loose and not packed against each other. However, in very localized areas of close proximity between the tooth and bone, an X-ray dense extracellular matrix was seen between the tooth and the bone. There the dense tissue does not exhibit a fibrillar structure, although it is conceivable that the tissue is composed of densely packed collagen fibrils. Thus, compression might be transferred from the tooth to the alveolar bone directly through contact areas or indirectly through a condensed PDL extracellular matrix. However, in both cases, the compression is localized in distinct compression sites rather than a compression side or surface. An interesting question arises from this finding regarding the fate of the fibers that are no longer in between the tooth and the bone in the contact areas. Studies show that collagen fibers are most suitable to function in tension and might be elongated 50% or more from the initial stage (12, 24). As no significant changes were observed in the collagenous networks before and after loading in the tension side, it is not clear whether tension of the collagen fibers transmits a significant tensional force to produce any deformation of the bone at these force levels. It is noteworthy to mention that during physiological vertical loading, the collagen fibers were notably stretched and arranged in parallel oblique stacks (3).

Conclusions

This study elucidates the mechanism underlying the first stages of the orthodontic movement of a multirooted tooth, minutes after load application. We show that:

- Direct contact areas between the tooth and the bone occur under orthodontic loads. The bony furcation serves as the limiting factor of the tooth displacement and therefore clearly shows why different levels of orthodontic forces result in the same extent of tooth movement. We suggest that the furcation area serves as the main force bearing area and thus might serve as a sensing and remodeling center throughout the orthodontic treatment.
- Whole body translational movement of a multirooted tooth, at least in the initial stages of an orthodontic movement, does not occur due to the contacts generated between the tooth and bone at the furcation.
- We demonstrate that under orthodontic forces, the PDL collagen fibers do not radically change their overall structure, neither in the so called tension side nor in the compression side which might lead to some questions regarding the existence of bone bending due to stretching of the collagen fibers. We do show that at least in the initial stages of an orthodontic movement compression is generated in the PDL. The site of compression is, however, localized and specific to the furcation area and the cervical region of the tooth.

Clinical relevance

The current knowledge on orthodontic tooth movement is based mainly on single-rooted tooth models. A multirooted tooth is significantly different from a single-rooted tooth, and therefore, our understanding of the mechanisms underlying multirooted tooth movement is deficient. This study shows that the furcation area is a major contributor to tooth movement both in direction and extent. Moreover, by elucidating the mechanisms underlying tooth movement, we address basic concepts in orthodontics such as the correlation between tooth movement and force, as well as PDL collagen network changes.

Acknowledgements: This research was funded by Israel Science Foundation Grant Number 407/10. S.W. holds the Dr. Walter and Dr. Trude Borchardt Professorial Chair in Structural Biology.

References

1. Storey E. The nature of tooth movement. *Am J Orthod* 1973;63:292–314.
2. Naveh GRS, Lev-Tov Chattah N, Zaslansky P, Shahar R, Weiner S. Tooth-PDL-bone complex: response to compressive loads encountered during mastication -A review. *Arch Oral Biol* 2012;57:1575–84.
3. Naveh GRS, Brumfeld V, Shahar R, Weiner S. Tooth periodontal ligament: direct 3D microCT visualization of the collagen network and how the network changes when the tooth is loaded. *J Struct Biol* 2013;181:108–15.
4. Naveh GRS, Brumfeld V, Dean M, Shahar R, Weiner S. Direct microCT imaging of non-mineralized connective tissues at high resolution. *Connect Tissue Res* 2014;55: 52–60.
5. Oppenheim A. Tissue changes, particularly of the bone, incident to tooth movement. *Eur J Orthodont* 2007;29:i2–15.
6. Meikle MC. The tissue, cellular, and molecular regulation of orthodontic tooth movement: 100 years after Carl Sandstedt. *Eur J Orthodont* 2006;28:221–40.
7. Sandstedt C. Einige Beitrage zur Theorie der Zahnregulierung. *Nordisk Tandlak Tidskr* 1904;5:126–56.
8. Baumrind S. A reconsideration of the propriety of the 'pressure-tension' hypothesis. *Am J Orthod* 1969;55:12–22.
9. Mühlemann HR. Tooth mobility. *J Periodontol* 1954;25:128–37.
10. Gottlieb B. Some orthodontic problems in histologic illumination. *Am J Orthod Oral Surg* 1946;32:113–33.
11. Naveh GRS, Shahar R, Brumfeld V, Weiner S. Tooth movements are guided by specific contact areas between the tooth root and the jaw bone: a dynamic 3D microCT study of the rat molar. *J Struct Biol* 2012;177:477–83.
12. Danz JC, Dalstra M, Bosshardt DD, Katsaros C, Stavropoulos A. A rat model for orthodontic translational expansive tooth movement. *Orthod Craniofac Res* 2013;16:223–33.
13. Ren Y, Maltha JC, Kuijpers-Jagtman AM. The rat as a model for orthodontic tooth movement—a critical review and a proposed solution. *Eur J Orthodont* 2004;26:483–90.
14. Nanci A. *Ten Cate's Oral Histology*, 6th edn. St. Louis, Missouri: Mosby; 2003.
15. Gibson JM, King GJ, Keeling SD. Long-term orthodontic tooth movement response to short-term force in the rat. *Angle Orthod* 1992;62:211–5.
16. Von Böhl M, Maltha J, Von den Hoff H, Kuijpers-Jagtman AM. Changes in the periodontal ligament after experimental tooth movement using high and low continuous forces in beagle dogs. *Angle Orthod* 2004;74:16–25.
17. Van Leeuwen EJ, Maltha JC, Kuijpers-Jagtman AM. Tooth movement with light continuous and discontinuous forces in Beagle dogs. *Eur J Oral Sci* 1999;107:468–74.
18. Walker CG, Ito Y, Dangaria S, Luan X, Diekwisch TG. RANKL, osteopontin, and osteoclast homeostasis in a hyperocclusion mouse model. *Eur J Oral Sci* 2008;116:312–8.
19. Reitan K. Some factors determining the evaluation of forces in orthodontics. *Am J Orthod* 1957;43:32–45.
20. Field C, Ichim I, Swain MV, Chan E, Darendeliler MA, Li W, et al. Mechanical responses to orthodontic loading: a 3-dimensional finite element multi-tooth model. *Am J Orthod Dentofacial Orthop* 2009;135:174–81.
21. Tanne K, Nagataki T, Inoue Y, Sakuda M, Burstone CJ. Patterns of initial tooth displacements associated with various root lengths and alveolar bone heights. *Am J Orthod Dentofacial Orthop* 1991;100:66–71.
22. Jeon PD, Turley PK, Moon HB, Ting K. Analysis of stress in the periodontium of the maxillary first molar with a three-dimensional finite element model. *Am J Orthod Dentofacial Orthop* 1999;115:267–74.
23. Rudolph DJ, Willes MG, Sameshima GT. A finite element model of apical force distribution from orthodontic tooth movement. *Angle Orthod* 2001;71:127–31.
24. Pins GD, Huang EK, Christiansen DL, Silver FH. Effects of static axial strain on the tensile properties and failure mechanisms of self-assembled collagen fibers. *J Appl Polym Sci* 1997;63:1429–40.